JOURNAL OF MECHANICAL ENGINEERING AND SCIENCES (JMES)
ISSN: 2289-4659 e-ISSN: 2231-8380
VOL. 16, ISSUE 4, 2022, 9253 – 9268
DOI: https://doi.org/10.15282/jmes.16.4.2022.08.0732

ORIGINAL ARTICLE

Relative assessment of various annular fin shapes for heat transfer and pressure penalty

M. Shah, R. Shah*

Department of Mechanical Engineering, Sardar Vallabhbhai National Institute of Technology, Surat, 395007, Gujarat, India
Phone: 0261-2204785

ABSTRACT – Three dimensional numerical investigations are carried out to analyse the effect of different shapes of annular fin on heat transfer characteristics and pressure drop across a tube surface. Shear stress transport based *k-ω* turbulence model is used to analyse flow physics and heat transfer characteristics in flow domain. Weak zones of heat transfer across a circular tube surface are identified for 2500 < *Re* < 13000. Three different shapes of annular fin are considered to test the possibility of optimum heat transfer characteristics in weak zones. Results are compared with circular shape annular fin. Circular shape annular fin outperforms in terms of overall rate of heat transfer at the cost of highest pressure drop. The heat transfer rate decreases by 18%, 21% and 31% in sectorial fin, elliptical fin and sectional fin as compared to that of circular fin at 12965 Reynolds number, but at other end pressure drop across a tube surface in case of these fins also decrease as compared to that of circular annular fin. Potential rate, ratio of heat transfer rate to required pumping power, is calculated to evaluate optimum fin performance. Potential rate of an elliptical fin is highest among all the reported cases.

ARTICLE HISTORY
Received: 18th July 2022
Revised: 07th Oct. 2022
Accepted: 17th Nov. 2022
Published: 27th Dec. 2022

KEYWORDS
Turbulence
Heat transfer
Forced convection
Potential rate

INTRODUCTION

Cross flow annular finned tube heat exchangers have major application in thermal power plant and processing industries. A good understanding of flow physics across a tube surface is important for thermal design of such heat exchangers. The transverse flow over a tube surface exhibits complex flow pattern. Region of flow attachment and flow separation near tube surface determines heat transfer characteristics, especially when the heat transfer occurs by mode of convection. Many researchers conducted experimental and numerical studies to understand the flow behaviour and thermal characteristics for a cross flow over heated circular cylinder for various range of Reynolds number. Scholten and Murray [1] experimentally investigated transient heat flux and local velocity magnitude near surface of tube in cross flow arrangement. Stagnant region in flow domain at upstream of tube and wake region due to separation of fluid molecules at downstream of tube were captured and effect of flow phenomena on heat transfer characteristics has been reported. It was concluded that the wake region formed at the downstream of the tube has major impact on heat transfer across tube surface. Forced convection phenomena across a tube surface was investigated numerically by Ooi et al. [2]. Angular heat transfer characteristics over tube surface were obtained experimentally. It was observed that the rate of heat transfer in upstream of tube surface is higher compared to that of downstream. Baranyi et al. [3] observed that change in momentum of air molecules near upstream and downstream region plays vital role convection heat transfer from the tube surface. It was reported that the coefficient of heat transfer is very low in region, top and bottom surface of tube, where flow separation begins.

In general, an augmentation in heat transfer rate can be achieved by intensifying the heat transfer coefficient or by enhancing the turbulence in flow near surface. In cross flow heat exchanger when tube side fluid is liquid and tube over fluid is air, rigorous air thermal resistance due to lower thermal conductivity and heat transfer coefficient is of prime concern [4–9]. Applying an annular extended surface to a circular tube is the most common and convenient way to reduce the thermal resistance on the air side. Tang and Yang [10] carried out numerical and experimental investigation to examine the thermal performance of single row finned tube arrangement. It was concluded that usage of extended surface is the effective way to reduced air side thermal resistance. Gionolio and Cuti [11] carried out experimental investigations to analyse heat transfer characteristics across a finned tube cross flow heat exchanger. Superior thermal performance with intensive pressure penalty was reported. Change in geometrical parameters of heat exchanger also invites the variation in thermal performance. Analysis of different design parameters is vital to intensify the overall performance of heat exchanger. Watel et al. [12], Mon and Gross [13], Sheu and Tsai [14], Bilirgen et al. [15] and Taler [16] investigated effect of change in design parameters of heat exchanger i.e. fin pitch, tube diameter and frontal air velocity on heat transfer and flow characteristics. Watel et al. [12] performed sets of experiment to investigate the effect of change in fin spacing and frontal velocity on overall heat transfer coefficient of cross flow annular fin-tube heat exchanger. It was concluded that influence of fin spacing on boundary layer becomes weak as the fin spacing exceeds about twice of boundary layer thickness. It was also concluded that boundary layer thickness near to fin and tube surface decreases with increase in frontal velocity. In a same way, Mon and Gross [13] investigated the heat transfer characteristics and flow pattern for

*CORRESPONDING AUTHOR | R. Shah | ✉ rds@med.svnit.ac.in

different fin pitch and Reynolds number through numerical analysis. It was concluded that the rate of heat transfer can be improved by increasing the number of fins but at the cost of intensive operating pressure. Bilirgen et al. [15] also carried out numerical investigation to analyse the effect of change in fin height, fin spacing and frontal velocity on heat transfer characteristics and overall performance of heat exchanger. It was concluded that the effect of change in fin thickness on heat transfer and flow characteristics is very less than fin height and spacing. Taler [16] also analysed fin tube heat exchangers having two rows of tube. Heat transfer and flow characteristics were analysed numerically as well as experimentally. Flow physics between two fins and effect of change in tube pitch in staggered arrangement on heat transfer and flow characteristics are discussed in detail. It was concluded that the design parameters of tube bank i.e. arrangement of tubes, pitch of fin and frontal velocity affect the heat transfer characteristics across a tube surface. Chen et al. [17] also investigated the effect of variation in fin spacing and frontal velocity on overall heat transfer characteristics. The average heat transfer coefficient was observed to increase with increase in air velocity and fin spacing, but when it comes to friction factor, heat transfer coefficient is highest at lowest air velocity in cases of highest fin spacing in reported range of fin-tube arrangement.

The overall performance of annular fin is affected due to variation in flow characteristics across a circular tube. Ooi et al. [2] and Schuz and Kottke [18] reported higher rate of heat transfer with intensive pressure gradient in stagnant region at upstream of tube in their analysis. Kundu and Das [19-20] investigated the effect of change in fin eccentricity and other geometrical parameters on overall performance of fin-tube arrangement. Variation in heat transfer characteristics is observed due to change in orientation of annular fin on tube surface. Semi analytical method was used to analyse the performance of elliptical fin [20]. An annular fin for different axis ratio was investigated. Efficiency and effectiveness of fin were calculated by predicting fin volume and rate of heat transfer. Numerical investigations were carried out by Farouk et al. [21] to investigate the effect of eccentricity along with variation in fin density and frontal velocity. Heat transfer coefficient on fin surface, fin efficiency and pressure drop were evaluated different values of Reynolds number. It was established that the eccentric annular fin with less dense fin arrangement is more efficient than concentric structure for reported range of Reynolds number. Benmachiche et al. [22] also compared the overall performance of eccentric and concentric structure. It was concluded that eccentric arrangement of fin in tube surface outperforms in terms of heat transfer and flow characteristics as compared to that of concentric arrangement of fin on tube. Geometrical parameters of annular fin affect the heat transfer and flow characteristics across a tube surface. Shah and Shah [23] and Nemati et al. [24] also analysed the effect of change in diameter ratio of fin on heat transfer and flow characteristics across a tube surface. It was concluded that geometrical parameters of fin affect the heat transfer and pressure drop.

Overall rate of heat transfer across a tube surface also can be enhanced by increasing the turbulence intensity in nearby region of circular tube. Perforated annular fin was used by Banerjee et al. [25] and Lee et al. [26] during their analysis to enhance the turbulence intensity in nearby region of circular tube. Lee et al. [26] experimentally investigated the heat transfer and flow characteristics near to finned tube surface. Effect of variation in perforation angle and number of perforations on heat transfer coefficient and pressure drop were investigated. It was concluded that fin improves heat transfer with higher pressure penalty as compared to that of plain fin-tube surface. Use of annular fin as a solution to enhance the thermal performance across a tube surface is general. Use of extended surface results in additional material requirement and higher pressure penalty. These add to the fixed and operating cost of the heat exchanger. To achieve optimum fixed cost, extended surface shape should be effective, and it should be placed in region of relatively low heat transfer coefficient. One way to reduce pressure drop is to use fin shape which creates low flow obstruction. Traditional methods of heat transfer augmentation using circular annular fin over tubes results in high pressure penalty. This is due to the fact that circular fin shape offers flow resistance at windward and produce wake zone at leeward surface of tube which increases the operating cost of heat exchanger. Thus, there is a need to test the various shapes of annular fin for optimum heat transfer with low pressure penalty. Three different shapes of annular fin are developed, and their heat transfer and flow characteristics are investigated and compared for 2500 to 13000 Reynolds number range in present study.

COMPUTATIONAL MODELING AND FORMULATION

Modeling of Computational Domain

Three dimensional numerical investigations are carried out for circular tubes of 0.025 m diameter, D and 0.003 m length. Numerical investigation is initiated with calculation of heat transfer characteristics for the case of smooth surface of circular tube. The enhancement in heat transfer by increasing contact area between two working mediums with negligible pressure penalty is the main motive of this investigation. Contact area is increased effectively by using fins. The annular (circular) fins having 0.052 m diameter, D_f, 0.001 m thickness, T_f and at spacing, S_f of 0.003 m are considered on surface of circular tube in second case. Figure 1 represents the cut section of annular finned tube geometry. In the third case, sectional fin with same design parameter is attached with tube surface. In the fourth case, sectional fin shape is replaced by sectorial one. In fifth case, heat transfer and flow characteristics are calculated for elliptical fin with 0.052 m vertical diameter (along fluid flow) and 0.034 m horizontal diameter (normal to fluid flow) [23]. Schematic views of different annular fins is shown in Figure 2. Fin geometries are differentiated by varying area of fin which is described in Table 1.

Computational domain for current investigation is presented in Figure 3. The upstream and downstream boundaries are located at 5 and 10 times of tube diameter respectively. The top boundary is located at 6 times of tube diameter. Fins are made of aluminium. The fluid flowing over the finned tubes is air. The properties of air are considered at 300 K initially.

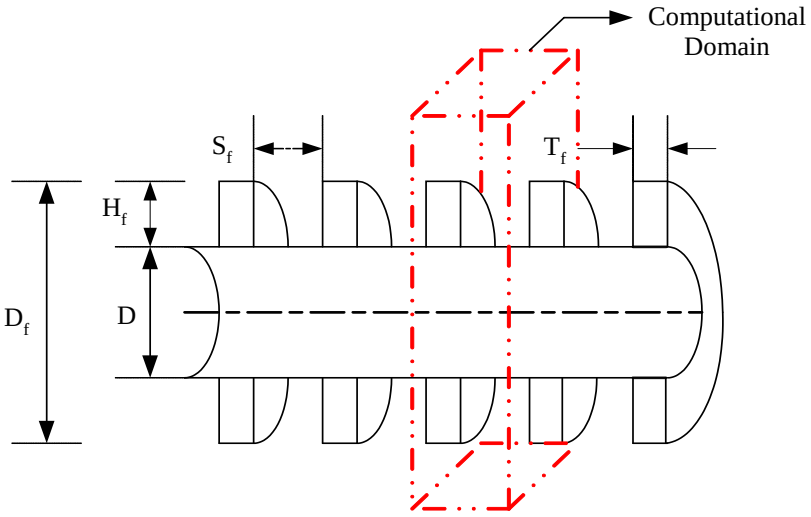

D_f = 0.052 m, D= 0.025 m, H_f = 0.0135 m, S_f = 0.003 m and T_f = 0.001 m

Figure 1. Cut-section of circular finned tube

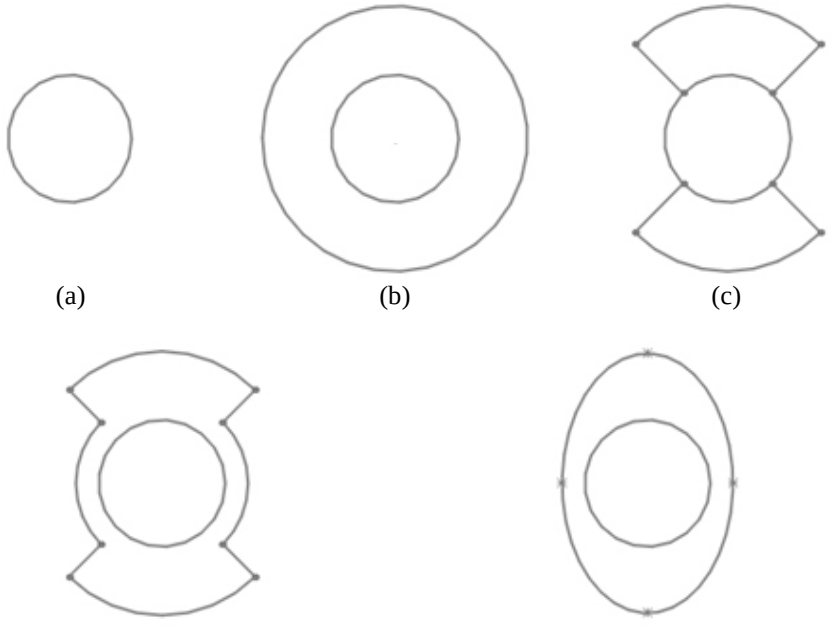

Figure 2. Schematic view of (a) smooth tube surface, (b) circular finned tube, (c) sectional finned tube, (d) sectorial finned tube and (e) elliptical finned tube

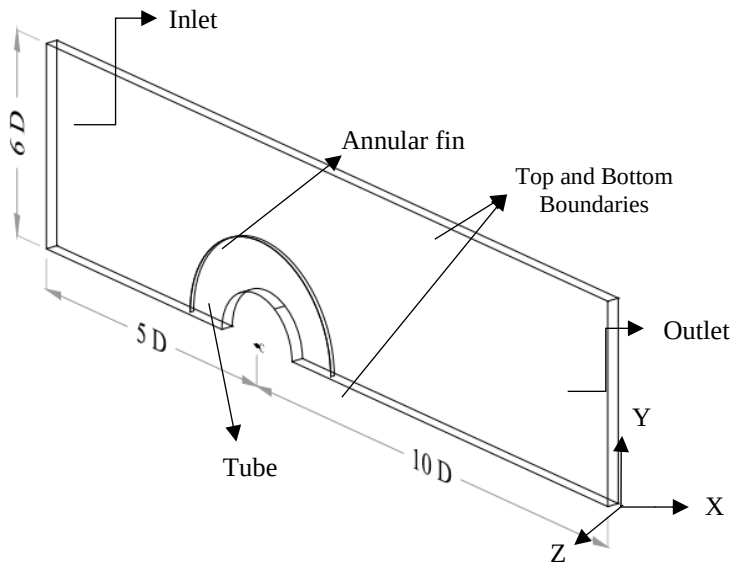

Figure 3. Computational domain

Table 1. Different geometrical cases of annular fin

Sl. No.	Type of Fin	Area ratio ($A_r = A_f/A_{cf}$) A_f = Fin area and A_{cf} = Circular fin area
1	Circular fin	1
2	Sectional fin	0.5
3	Elliptical fin	0.55
4	Sectorial fin	0.75

Governing Equations

Three dimensional, incompressible, steady, and turbulent flow is considered in current investigation. The governing equations for mass, momentum, energy, and turbulence are considered as follows:

Continuity equation:

$$\frac{\partial u_i}{\partial x_i} = 0 \tag{1}$$

Momentum equation:

$$\frac{\partial}{\partial x_j}(u_i u_j) = -\frac{1}{\rho}\frac{\partial p}{\partial x_j} + \frac{\partial}{\partial x_j}\left[\vartheta\left(\frac{\partial u_i}{\partial x_j} + \frac{\partial u_j}{\partial x_i} - \frac{2}{3}\delta_{ij}\frac{\partial u_l}{\partial z}\right) - \overline{u_i' u_j'}\right] \tag{2}$$

where,

$$-\overline{u_i' u_j'} = \vartheta_{trb}\left(\frac{\partial u_i}{\partial x_j} + \frac{\partial u_j}{\partial x_i} - \frac{2}{3}\delta_{ij}(\rho k + \mu_t\frac{\partial u_i}{\partial x_i})\right) \tag{3}$$

Governing equation of turbulent kinetic energy (k) and specific dissipation rate (ω) is described as:

$$\frac{\partial}{\partial x_j}(u_j k) = P_x - \beta_1 \rho k\omega + \frac{\partial}{\partial x_j}\left[(\mu + \frac{\mu_{turb}}{\sigma_k})\frac{\partial k}{\partial x_j}\right] \tag{4}$$

$$\frac{\partial}{\partial x_j}(u_j \omega) = A\rho S^2 - \beta_2 \rho\omega^2 + \frac{\partial}{\partial x_j}\left[(\mu + \frac{\mu_{turb}}{\sigma_k})\frac{\partial \omega}{\partial x_j}\right] + 2(1-F_1)\frac{\rho}{\sigma_\omega \omega}\frac{\partial k}{\partial x_i}\frac{\partial \omega}{\partial x_i} \tag{5}$$

Energy equation:

$$\frac{\partial}{\partial x_i}(u_i(\rho E + p)) = \frac{\partial}{\partial x_i}(k_{ff}\frac{\partial T}{\partial x_i}) \tag{6}$$

where E is the gross energy and $k_{ff} = k + k_{turb}$., k_{turb} is noted as turbulent thermal conductivity.

Conduction occurs in solid portion of fin. Therefore, the following equation is used to investigate energy transport.

$$\frac{\partial}{\partial x_i}\left(k_s \frac{\partial T}{\partial x_i}\right) = 0 \tag{7}$$

Boundary Condition

The air with 300 *K* enters from inlet boundary into the domain. Velocity inlet is assigned as a boundary condition on inlet surface. Inlet velocity is varied from 1 m/s to 10 m/s. At tube surface no slip along with constant temperature boundary condition is set. Fin domain is modeled as solid domain. Outer region to tube and fin is modelled as fluid domain. In solid domain, only energy Eq. (7) is solved to obtain temperature distribution. Top and bottom boundary of the domain are considered as symmetry. Pressure outlet as a boundary condition of 1 atm is set at domain outlet.

Meshing and Flow Modelling

Domain discretisation is vital stage of numerical investigation. Structured grid is generated in computational domain to investigate heat transfer and flow characteristics across a finned tube surface. Density of grid is varied by using the of successive ratio function. Fine grids are generated near tube and fin surface. In the region away from tube and fin surface, course grids are developed. Wall Y^+ near tube surface varies between 0.05 and 1.04 for $2500 < Re < 13000$. Figure 4 represents the front view of three-dimensional computational domain. Performance of four different geometries of an annular fin is investigated numerically and compared with bare circular tube. The simulations are performed for $2500 < Re < 13000$. *k-ω* turbulence model based on the theory of shear stress transport is used to analyse the thermal and flow properties across a circular tube using FLUENT. Pressure and velocity variables are coupled using SIMPLEC algorithm. Governing equations are solved using QUICK scheme. The criteria for convergence of mass and momentum conservation equations are set to 10^{-4} and 10^{-6} for energy conservation equation.

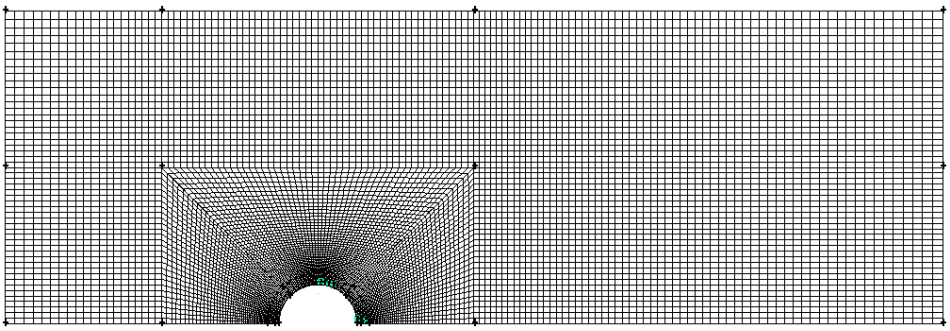

Figure 4. Orthographic view of formatted grid in computational domain

RESULTS AND DISCUSSION

In present study, the effect of different annular extended surface on heat and flow characteristics across a tube surface is investigated for 2500 to 13000 Reynolds number range. Four different shapes of annular extended surface are investigated, and pressure drop is considered as a parameter to do grid independence study. Flow physics across a tube surface varies due to change in shape of annular fin. As it is discussed the importance of grid generation in numerical investigation, it is interesting to find out the appropriate number of elements with which the numerical results will not be altered significantly (not more than 5%). In present study five different finned tube cases are considered. Therefore, the number of elements in grid independence stage are different for each case. Table 2 depicts the number of elements in grid independence stage for each case of finned tube considered in current investigation.

Table 2. Number of elements at grid independence stage

Sr. No.	Type of fin	Number of Elements
1	Smooth tube	15,18,840
2	Circular fin	16,00,344
3	Sectional fin	16,08,228
4	Sectorial fin	16,12,804
5	Elliptical fin	16,48,944

Figure 5 shows variation of the Numerically calculated average Nusselt number, *Nu* with *Re*. Numerically obtained *Nu* is compared with that obtained from empirical correlation. Empirical value of *Nu* is obtained using,

$$Nu = 0.3 + \frac{0.62\, Re^{0.5} Pr^{0.33}}{[1 + (0.4/Pr)^{0.66}]^{0.25}} [1 + \left(\frac{Re}{282000}\right)^{0.625}]^{0.8} \quad (8)$$

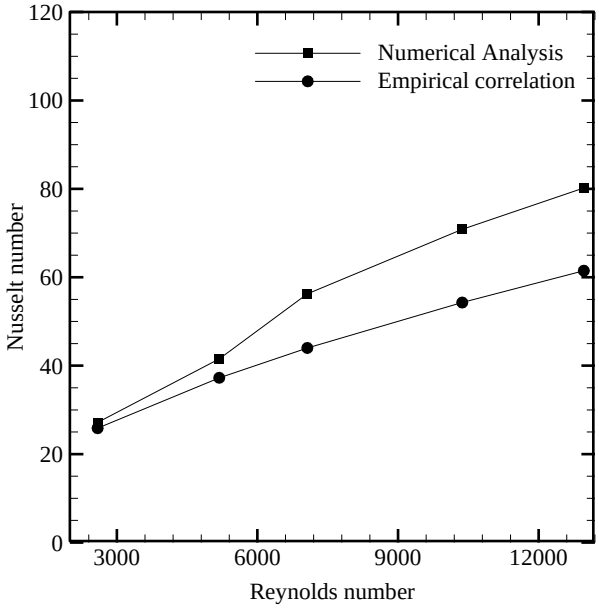

Figure 5. Variation of average Nusselt number

Empirical Eq. (8) is developed based on data obtained from sets of experiments [27]. It was reported that value of *Nu* obtained from Eq. (8) will deviate by 30% [27]. Comparison of numerical *Nu* and empirical *Nu* shown in Figure 5 indicates that at low *Re* the difference between two values is low compared to high *Re*. At low *Re* deviation of 6% is observed while at higher *Re* maximum offset is 14%. These difference in values of *Nu* are well within accuracy of the empirical Eq. (8).

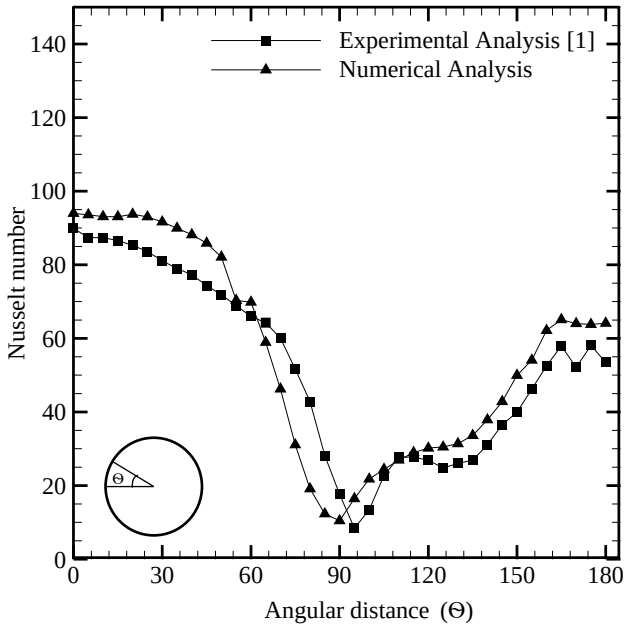

Figure 6. Validation of local Nusselt number

Value of local Nusselt number (at various angular position) across a circular tube surface is also compared with that of reported experimentally by Scholten and Murray [1]. Figure 6 compare numerically obtained local Nusselt number with experimental one [1] at 7060 Reynolds number. Trend of variation in local Nusselt number are comparable. As

shown in Figure 6, present study overestimates the Nusselt number. Nusselt number values are deviating by 4% at upstream of tube surface. Deviation in result increases at downstream of tube surface. There is a deviation of 11% in Numerical Nusselt number at downstream surface of tube. Scholten and Murray [1] used thermocouples to measure temperature at angular position on circular tube surface. Fluid flow characteristics in upstream and downstream region of tube is more complex because of formation of stagnant and wake region respectively. Use of thermocouples, to measure the tube surface temperature, disturbs the flow regime which changes the flow physics and heat transfer characteristics near surface.

Flow Behaviour

Overall objective of current numerical investigation is heat transfer enhancement with optimum pressure penalty across a tube surface. Numerical investigations are carried out for four different geometries of extended surfaces. Relative assessment is carried out for $2500 < Re < 13000$. Figure 7 represents the velocity contours of each geometrical case at 2590 and 12965 Reynolds number. Velocity contours and streamline plots are helpful to understand flow physics grossly. In Figure 7, Variation in velocity magnitude at mid of the domain on x-y plane (vertical plane: parallel to flow) is represented. As shown in Figure 7, circular tube offers obstruction to flow field. As fluid comes closure to windward tube surface, it has to change its direction to adjust the flow pattern as per the shape of obstruction also at tube surface fluid velocity should be relatively zero. This produces a region of velocity gradient, in which velocity varies from relatively zero to freestream velocity. Shape and size of region of velocity gradient is affected by geometry of obstruction and flow velocity. As shown in case of smooth cylinder, the region of velocity gradient at windward surface spreads in larger area at Re =12965 compared to that of Re =2960. Variation in region of velocity gradient also occurs due to change in fin type. This can be noticed with change in velocity contours at windward surface of tube for different fin type.

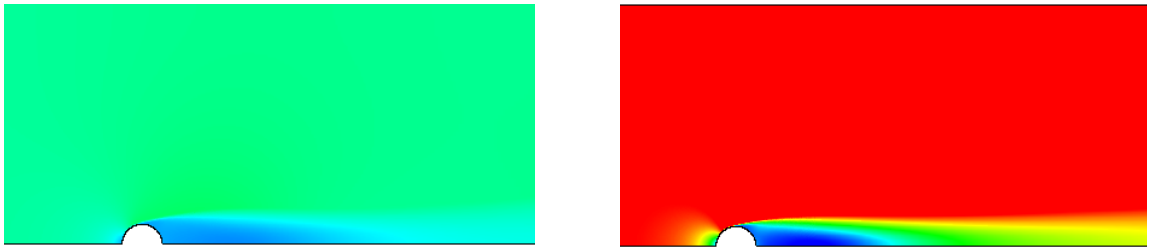

Case (A): Smooth circular tube ($A_r = 0$)

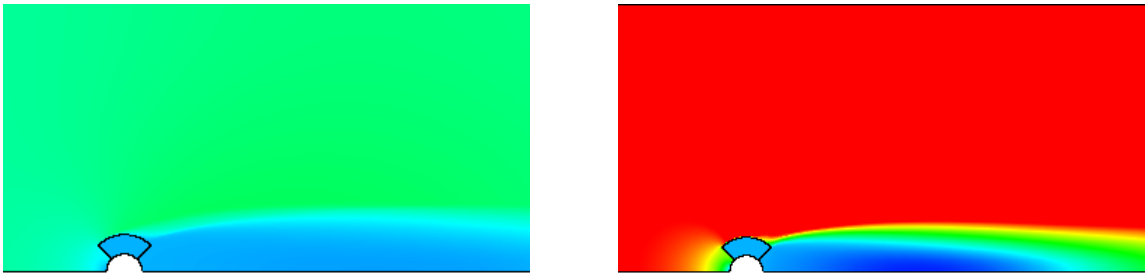

Case (B): Sectional finned tube ($A_r = 0.5$)

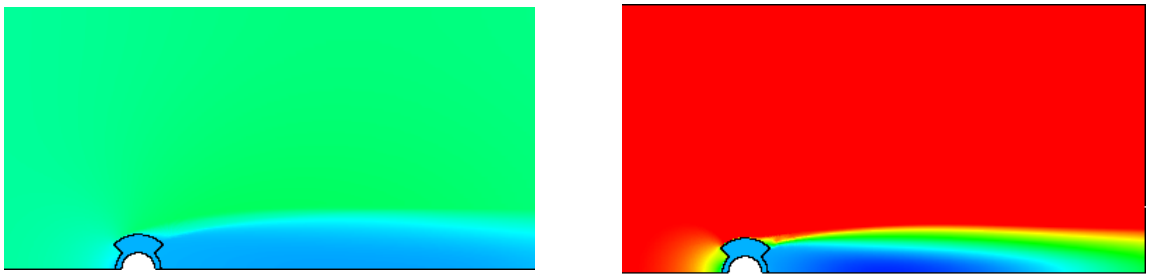

Case (C): Sectorial finned tube ($A_r = 0.75$)

Figure 7. Velocity contours on x-y plane

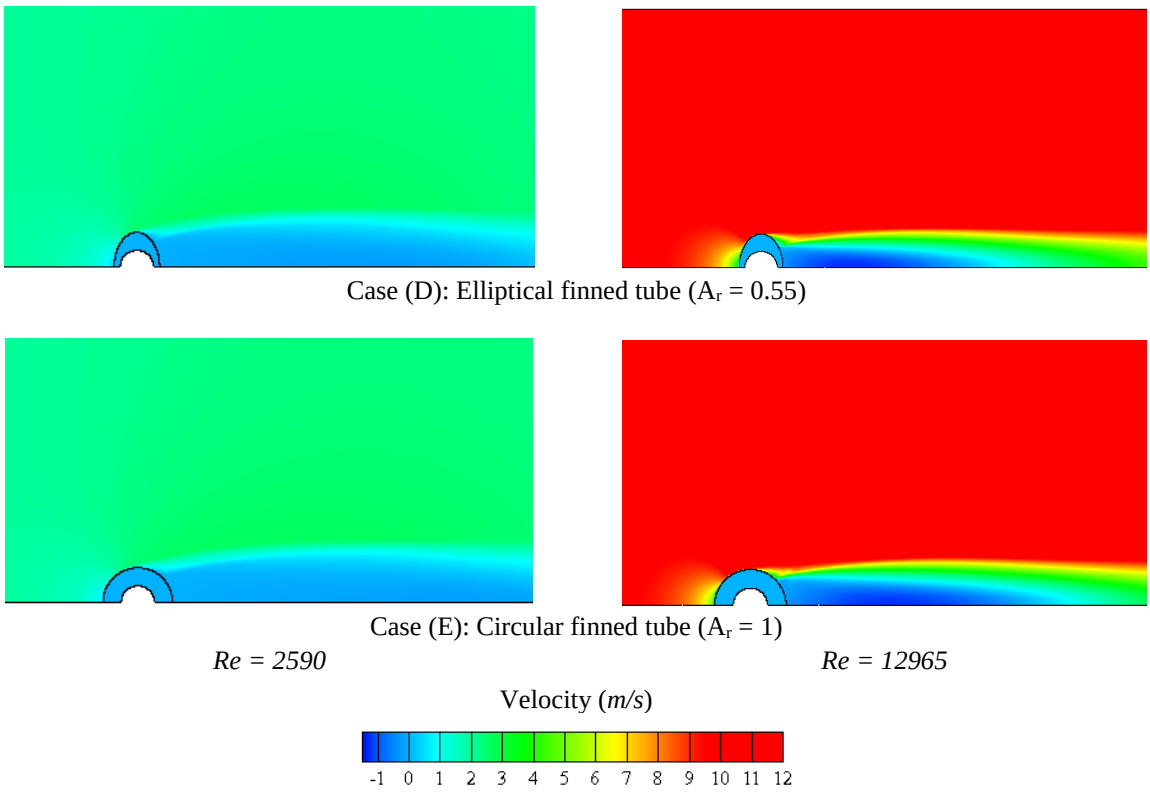

Figure 7. Velocity contours on x-y plane (cont.)

On the leeward surface of the tube, fluid streams separate from the surface. This flow separation creates region of negative pressure. Fluid particles exhibits negative velocity with tendency to recirculate in this region. It is generally referred as a wake region. The intensity of recirculation of fluid particles in wake region decide the heat transfer characteristics at leeward tube surface. The length of recirculation zone in wake region is larger at low Reynolds number. Intense recirculation zone, higher value of negative velocity, in wake region is captured at high Reynolds number for all cases reported. This can be observed by comparing velocity contours presented in Figure 7. The region of velocity gradient at windward surface of tube and wake region at leeward surface are more intensive in case of circular shape of annular fin. Similar kind of flow pattern is observed by Shah and Shah [23]. Analysis of flow characteristics between two fins are essential to understand the local flow behaviour over a finned tube surface. Figures 8 and 9 represent the velocity contours on z-x plane (horizontal plane: parallel to flow) and y-z plane (vertical plane: normal to flow) at different distances from the centre of tube. Figure 10 represents the streamline plot to understand flow physics in upstream and downstream of tube precisely. In Figure 10, streamline plots are captured on x-y plane at mid of the domain and on vertical symmetry plane for *Re* = 12965. Case 1 in Figure 8 shows velocity contours at vertical distance of 0.015 m from the centre of tube. Case 2 and 3 depict the velocity contour distribution at vertical distance of 0.02 m and 0.026

As shown in Figure 8, hydraulic boundary layer is formed near the fin surface as the flow passes over the finned tube surfaces. Formation of hydraulic boundary layer near a fin surface controls the flow characteristics near tube surface. As can be seen in Figure 7, shape and size of wake region on leeward surface varies with velocity and smaller wake zone was captured for smooth circular tube compared to tube with finned surfaces. As shown in case 1 in Figure 8, negligible variation in velocity magnitude exist in case of smooth circular tube at 0.015 m vertical distance from centre of tube. In case of smooth tube, height of wake zone is restricted near tube surface. At 0.015 m, z-x plane is just above this wake zone. Due to this variation in velocity is negligible. For other cases of finned tube surface, presence of fin is experienced by flow at 0.015 m. Presence of fin establish velocity gradient. On z-x plane velocity contour variation between two successive fin passage is different for various finned shapes. This variation can be easily identified at *Re* =12965. At *Re* =12965, for smooth tube surface (A_r=0) reduction in axial velocity is attributed to upward shift in flow due to presence of large wake zone as shown in case 1 of Figure 8. For finned tube surfaces this variation in velocity is occurring earlier compared to smooth tube surface. For sectorial, sectional and circular finned cases, reduction in axial velocity magnitude starts from the tube axis as shown in Figure 8 (Case1 at *Re*=12965). For elliptical finned tube reduction in velocity is observed at the trailing end of the passage formed between two fins. Region of flow deceleration in axial direction are highlighted and indicated as flow shift in Figure 8 (Case1 at *Re*=12965). This observed difference in location of flow deceleration and length of flow retardation dependence on wake region formed on leeward surface of tube and between the fin passage.

The wake regions formed on leeward side and between fin passage for different cases are shown in Figure 8. Figure 8(a) represents wake on plane passing through fin. Shape and size of wake regions formed in sectional, sectorial and circular fin is comparable. For elliptical fin wake region is smaller in length and height compared to other fin surfaces.

Figure 8 (b) represents wake on plane passing through mid of the fin passage. Compared to case of Figure 8(a), wake region effect is wider for all the geometrical cases reported. Smaller and week wake zone is present in case of elliptical fin case. Change in fin shape alter the strength, shape and size of week zone formed on leeward side of tube surface. This change alters the fluid flow regime over the fin and through fin passage. Larger and wider wake zone in sectorial, sectional and circular tube surface obstruct the axial flow and flow shifts upwards. Height of wake zone is maximum in case of sectional fin (A_r=0.5). This upward flow shifting results in axial flow retardation as shown in Figure 8.

Velocity contours on plane at distance of 0.02 m and 0.026 m indicates that flow deceleration is happening at the trailing edge of the fin near leeward surface of the tube. For elliptical fin case fluid is able to move through the fin passage with maximum flow velocity without any flow shift and flow deceleration. This due to fact that smallest wake zone has relatively week or no effect on flow regime at a distance of 0.02m and 0.026 m. As shown in case 2 and case 3, area of fin cut section varies as the shape of fin and height of z-x plane varies in y direction. In case of A_r = 0.55, width of fin is less as compared to that of other geometrical cases. In case 2, velocity contours of A_r = 0.55 shows that the fluid particles of incoming stream strike the wake region at higher velocity magnitude and decrease the dominance of wake region in downstream of tube. At other hand, in all other geometrical cases, fin surface covers the certain area of wake region and due to this the intensity of velocity magnitude of incoming fluid stream decreases before fin surface ends.

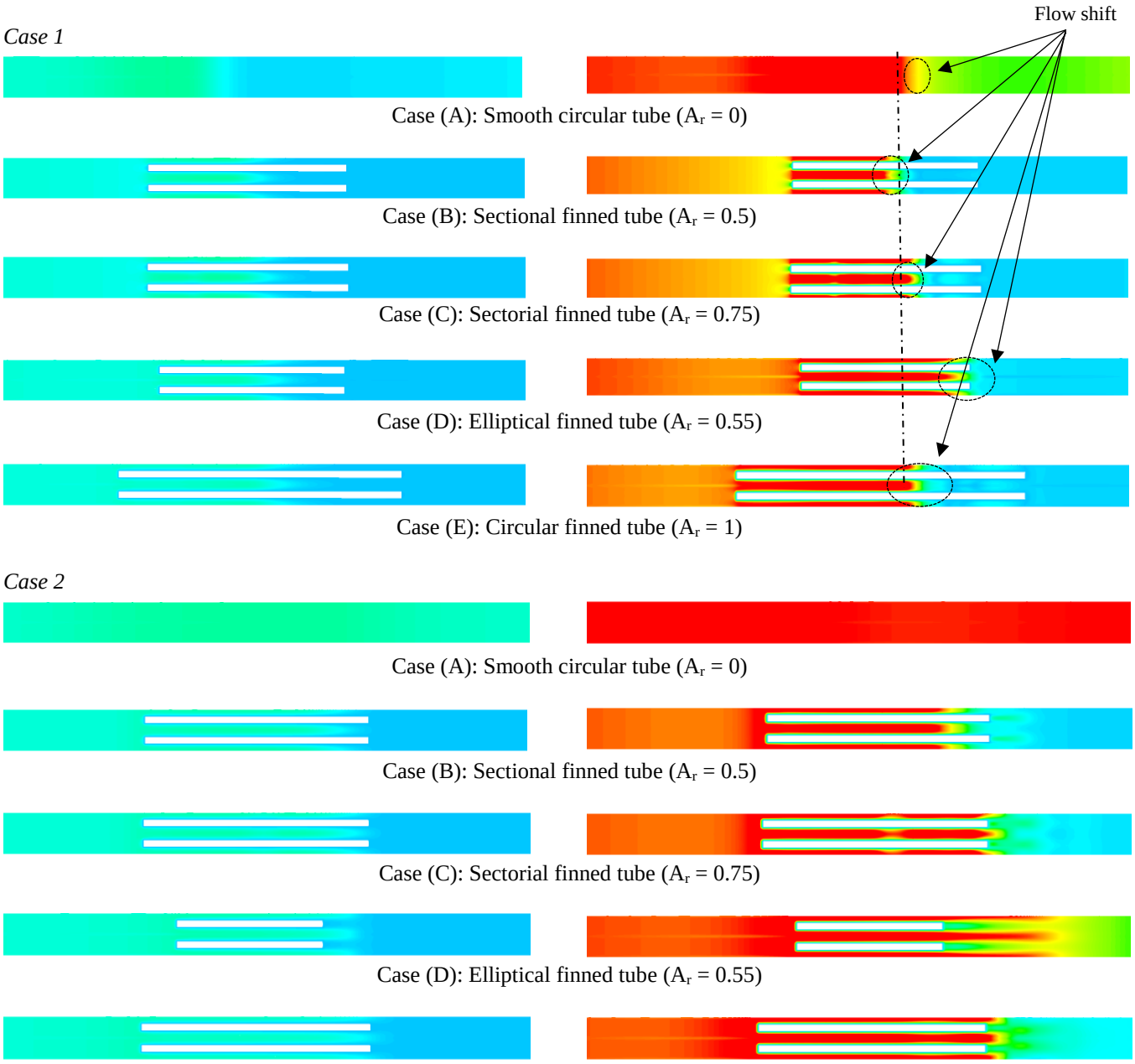

Figure 8. Velocity contours on z-x plane

Case 3

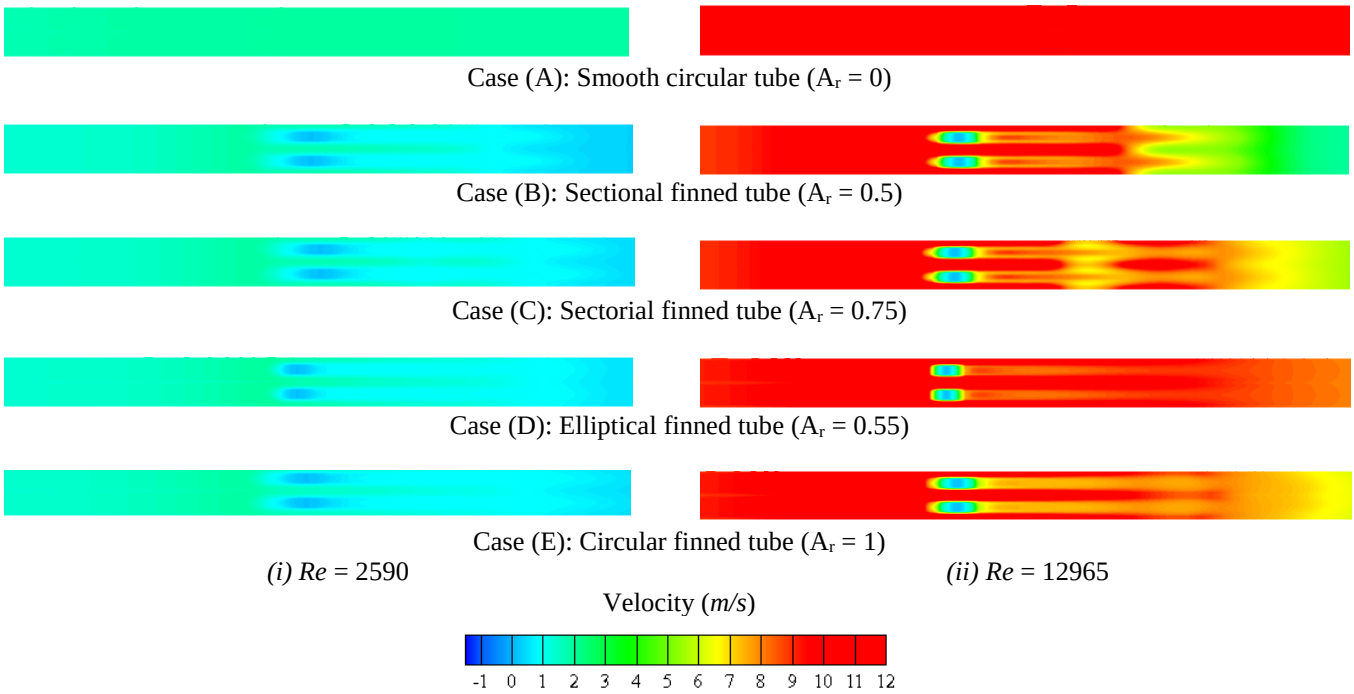

Figure 8. Velocity contours on z-x plane (cont.)

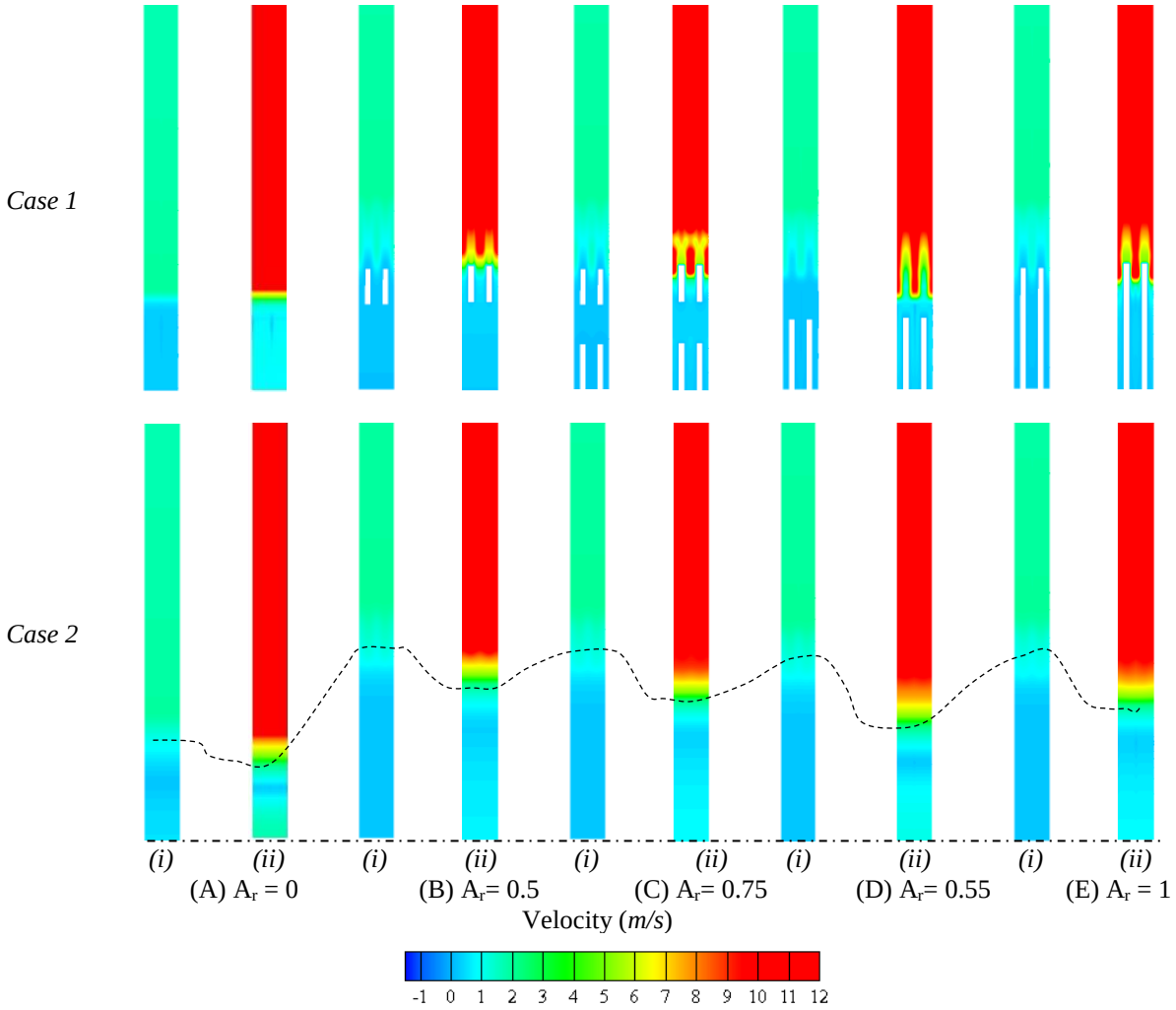

Figure 9. Velocity contours on y-z plane at *(i)* 2590 and *(ii)* 12965 Reynolds number

Figure 9 represents the velocity contours on y-z plane at two different Reynolds number and distance from centre of tube to understand the effect of wake region on flow field of incoming fluid particles at downstream in flow domain. Case 1 and 2 in Figure 9 represent the velocity contours on y-z plane at 0.015 m and 0.05 m distance (along the flow) from centre of tube at 2590 and 12965 Reynolds number. It can be read from Figure 9 that smaller area of wake region captured in case of smooth circular tube and maximum area of wake region is captured in case of sectional fin. In Figure 9 contours of maximum velocity is observed at larger vertical distance for sectional, sectorial and circular fin compared to elliptical fin. These indicate upward shifting of flow due to introduction of fin on tube surface. In case 2 of Figure 9 region of free stream velocity and region of velocity gradient due to presence of wake zone is separated by dotted line. The change in height of dotted line for different cases from tube axis is attributed to specific shape of wake region associated with fin shapes as shown in Figure 10.

Variation in temperature near surface is primary decides heat transfer characteristics of surface. Effect of velocity gradient and wake region on heat transfer characteristics can understood with temperature contours. Figure 11 represents the temperature contours at mid of the domain on x-y plane for all the geometrical cases at 2590 and 12965 Reynolds number. Air at certain freestream velocity approaches tube surface and divert upward. Convection heat transfer occurs due presence of fluid particles near surface. Fin shapes decides the shape, spread and strength of wake and velocity gradient regions. Also, the flow regime near fin surface and between fin passage is affected by these regions. Accordingly, the heat transfer characteristics vary. Temperature of fluid in wake region is high due to recirculation of fluid particles that occurs because of effect of negative pressure in that region. As it is previously discussed from Figure 7 that the wake region is larger at low Reynolds, impact of that on temperature variation in that region can be easily captured in Figure 11. As shown in Figure 11, high temperature zone behind the tube surface is larger in all the geometrical cases of an annular fin at low Reynolds number. The area of high temperature zone in each geometrical case decreases with increase in Reynolds number. The area of high temperature zone behind tube surface also varies because of variation in fin geometry at particular Reynolds number. Highly intensive and larger wake region is captured in case of circular fin through plotted velocity contours in Figure 7. The higher scale of temperature in flow region behind a circular fin reflects the effect of higher intensity of recirculation of fluid particles in that wake region.

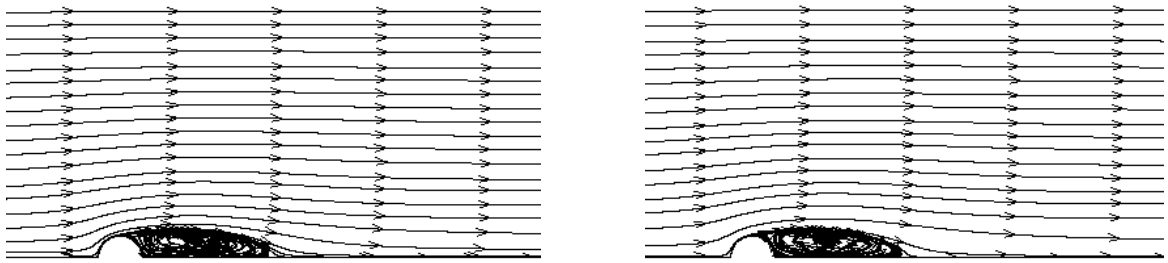

Case (A): Smooth circular tube (A_r = 0)

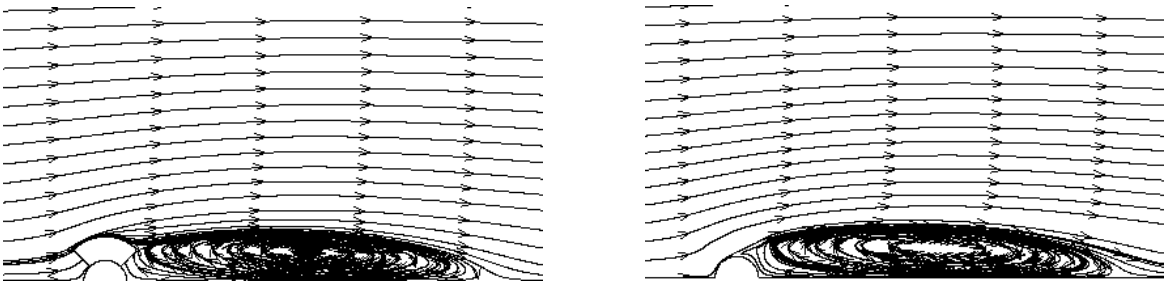

Case (B): Sectional finned tube (A_r = 0.5)

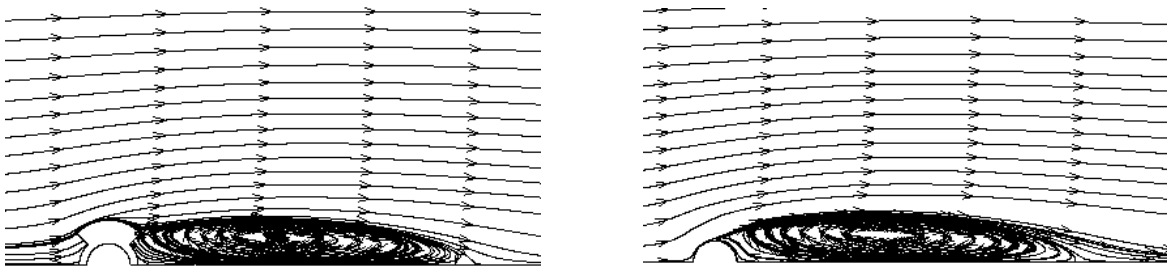

Case (C): Sectorial finned tube (A_r = 0.75)

Figure 10. Stream line plots at 12965 Reynolds number

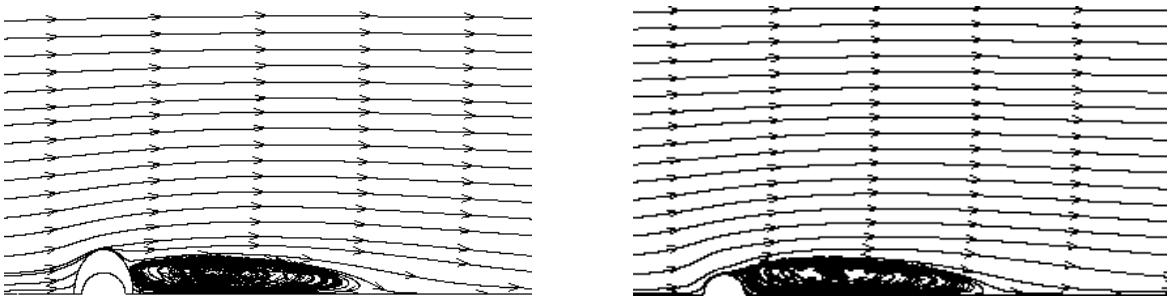

Case (D): Elliptical finned tube (A_r = 0.55)

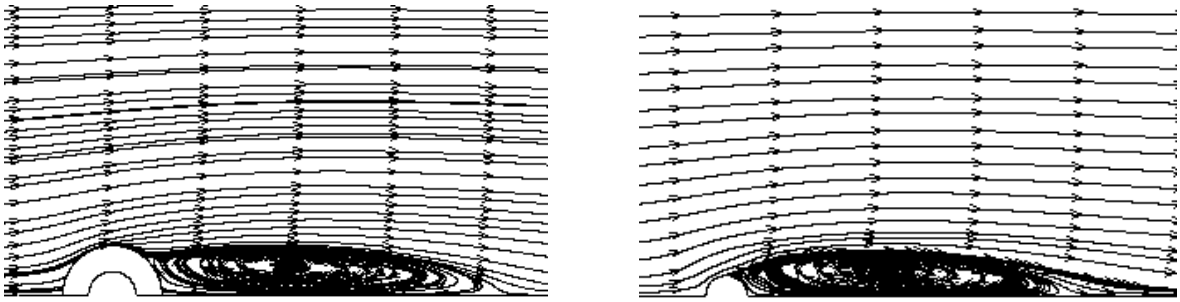

Case (E): Circular finned tube (A_r = 1)

Figure 10. Stream line plots at 12965 Reynolds number (cont.)

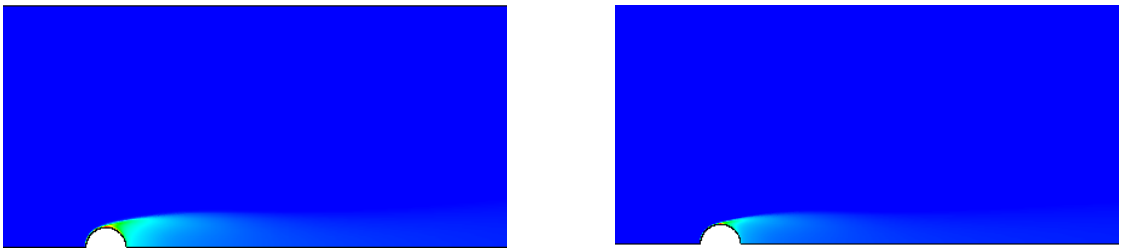

Case (A): Smooth circular tube (A_r = 0)

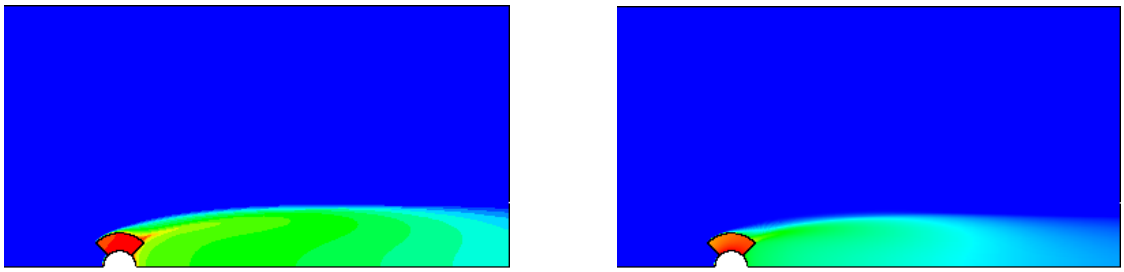

Case (B): Sectional finned tube (A_r = 0.5)

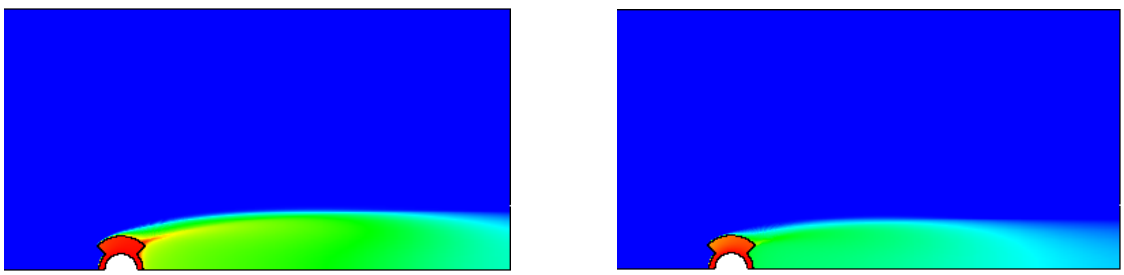

Case (C): Sectorial finned tube (A_r = 0.75)

Figure 11. Temperature contours

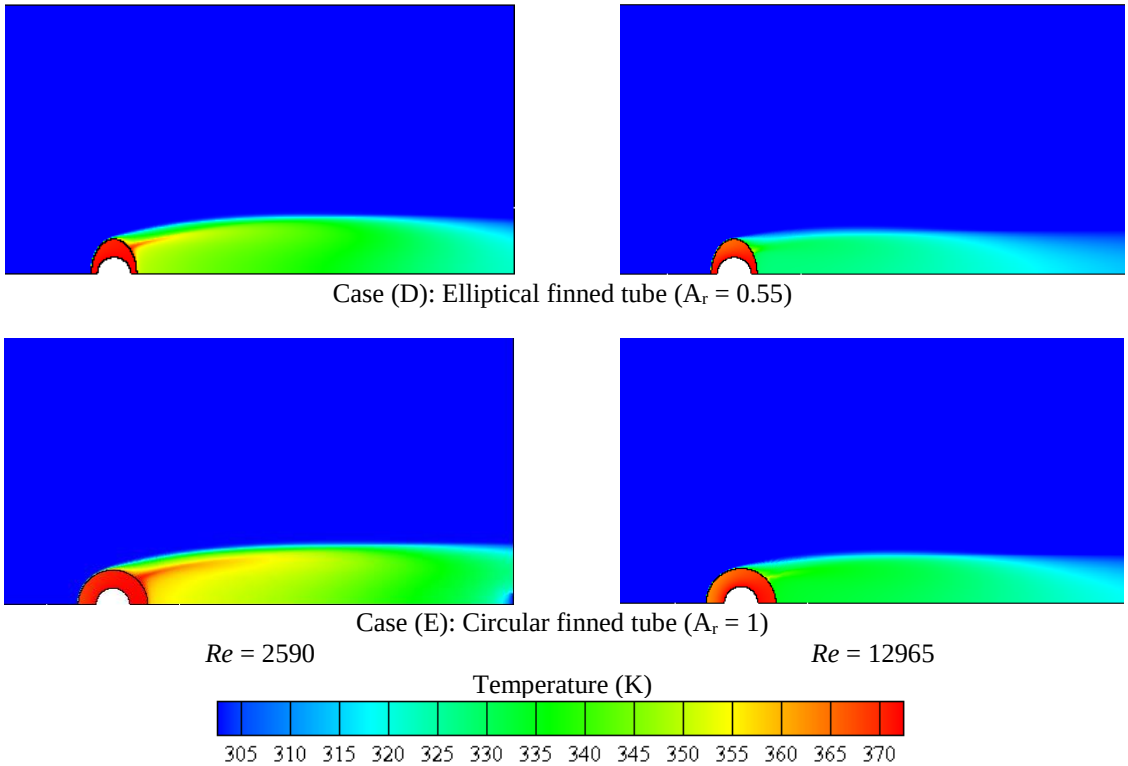

Figure 11. Temperature contours (cont.)

Calculation of Heat Transfer Coefficient and Pressure Penalty

Numerical investigations are carried out to analyse the effect of different shapes of an annular fin on heat transfer and flow characteristics across a tube surface. The relative assessment is carried out for 2500<*Re*<13000. Variation in overall rate of heat transfer due to change in area ratio of fin at different Reynolds number is shown in Figure 12. It can be observed that the overall rate of heat transfer increases due to increase in area ratio of fin. Highest rate of heat transfer is occurring for circular fin (A_r = 1) compared to other cases of annular fin due to availability of maximum heat transfer area. Heat transfer rate decreases in case of sectorial fin (A_r = 0.75) by 11%, in case of elliptical fin (A_r = 0.55) by 20% and in case of sectional fin (A_r = 0.5) by 21% compared to circular fin (A_r = 1) at 2590 Reynolds number. The lowest heat transfer rate is available with bare circular tube and is almost 90% lower compared to circular finned tube arrangement. At higher Reynolds number this difference becomes larger. Rate of heat transfer decreases by 18%,21% and 31% in case of sectorial fin, elliptical fin and sectional fin as compared to that of circular fin case at 12965 Reynolds number.

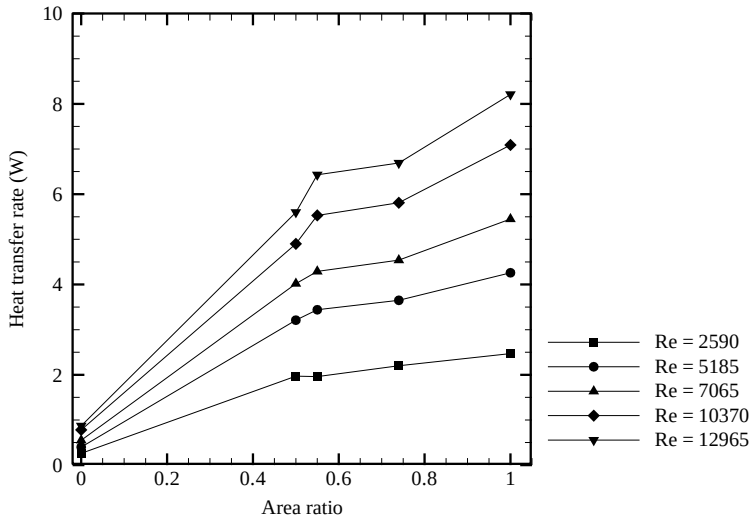

Figure 12. Heat transfer rate

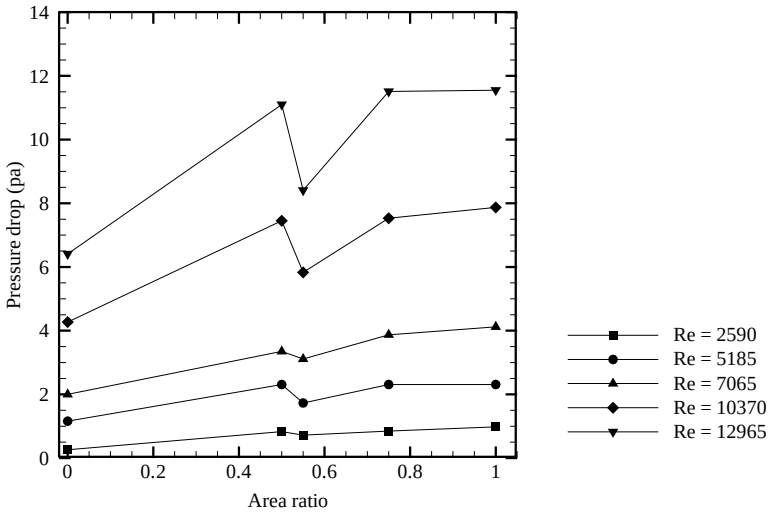

Figure 13. Pressure drop variation

The operating pressure is of great importance, since it is associated with pumping power. Figure 13 represents the pressure drop at particular operating condition for different cases of annular fin. It is observed that the increase in area ratio enhances pressure penalty. As shown in Figure 13, circular fin (A_r = 1) has a highest pressure penalty as compared to that of other geometrical cases of annular fin. Lowest pressure penalty is observed for elliptical fin case. Pressure penalty increases because of enlargement in wake zone. As per streamline pattern shown in Figure 10, larger wake zone is associated with circular, sectorial and sectional fin case. Maximum pressure drop is observed in case of circular fin (A_r = 1). Pressure drop decreases by 10%, 26% and 15% in case of sectorial fin (A_r = 0.75), elliptical fin (A_r = 0.55) and sectional fin (A_r = 0.5) respectively compared to circular fin (A_r = 1) case at 2590 Reynolds number. Lowest pressure drop is reported in case of bare circular tube surface for reported range of Reynolds number. At *Re* = 12965, the pressure penalty is low by 27% and 4% in case of elliptical fin and sectional fin compared to circular fin surfaces.

Calculation of Potential Rate

Concept of annular fin is used to improve the overall rate of heat transfer and it is observed that circular fin (A_r = 1) performs well in terms of increasing heat transfer rate. But the associated intensive pressure drop is considered as a crucial parameter. Hence it is required to investigate the potential rate of each fin for 2500 < *Re* < 13000. Figure 14 represents potential rate of different geometrical cases for reported range of Reynolds number. Potential rate is calculated by considering the ratio of heat flux to pumping power for unit cross-sectional area for a particular case. For all the geometrical cases, Reynolds number was increased by increasing approaching air velocity. As shown in Figure 13, Increasing range of Reynolds number increases the pressure penalty for all the cases. Therefore, pumping power increases with increase in Reynolds number that decreases the potential rate of particular case of fin surface. As shown in Figure 14, potential rate of elliptical finned tube arrangement is higher as compared to that of other geometrical cases for reported range of Reynolds number. As illustrated in Figure 12 and Figure 13, heat transfer rate is higher in case of circular finned tube arrangement as compared to other cases, but at the cost of highest pressure penalty. Therefore, the potential rate of circular fin decreases as compared to that of elliptical fin case.

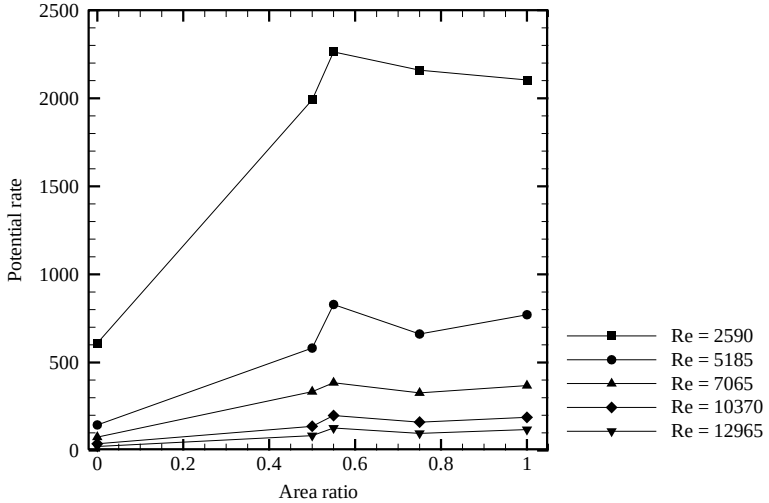

Figure 14. Variation of potential rate

Potential rate increases by 8% in case of elliptical fin and 3% in case of sectorial fin as compared to circular fin at 2590 Reynolds number. In case of sectional fin and bare cylinder at 2590 Reynolds number, potential rate decreases by 6% and 71% respectively as compared to that of circular fin case. Trend is changed as the Reynolds number increases. Elliptical fin has advantage of 9% increase in potential rate compared to circular fin. For other geometrical cases, potential rate is less as compared to circular fin at same Reynolds number.

CONCLUSION

Four different shapes of fins are evaluated numerically for heat transfer rate, pressure drop and potential rate. Performance is compared for heat transfer against pressure penalty. Based on present computational investigations the major findings are:

(1) Annular fin shape affects the shape, size, and strength of wake zone near leeward surface of bases tube. Wake zone governs the flow and heat transfer characteristics near fin surfaces. For optimum performance of finned tube surface wake zone dimensions should be comparable with that of tube without fin.

(2) The circular shape of annular fin is suitable for maximum rate of heat transfer at the cost of highest pressure penalty due to larger wake zone on leeward side of tube surface.

(3) The elliptical shape of annular fin outperforms in terms of potential rate. Heat transfer rate is moderate with lowest pressure penalty. This is due to the smallest wake zone captured for $2500 < Re < 13000$ compared to other fin shapes.

ACKNOWLEDGEMENT

We thank the Department of Mechanical Engineering, Sardar Vallabhbhai National Institute of Technology for the support and facilities provided.

REFERENCES

[1] J. W. Scholten and D. B. Murray, "Unsteady heat transfer and velocity of a cylinder in cross flow—I. Low freestream turbulence," *International Journal of Heat and Mass Transfer*, vol. 41, no. 10, pp. 1139–1148, 1998.

[2] A. Ooi, L. Aye, K. Szczepanik, A. Ooi, L. Aye, and G. Rosengarten, "A numerical study of heat transfer from a cylinder in cross flow," in *15th Australasian Fluid Mechanics Conference*, Sydney, Australia, 2004.

[3] L. Baranyi, S. Szabó, B. Bolló, and R. Bordás, "Analysis of low Reynolds number flow around a heated circular cylinder," *Journal of Mechanical Science and Technology*, vol. 23, pp. 1829–1834, 2009.

[4] C. C. Wang, W. S. Lee, and W. J. Sheu, "A comparative study of compact enhanced fin-and-tube heat exchangers," *International Journal of Heat and Mass Transfer*, vol. 44, no. 18, pp. 3565–3573, 2001.

[5] T. Perrotin and D. Clodic, "Fin efficiency calculation in enhanced fin and tube heat exchangers in dry condition," in *International Congress of Refrigeration*, Washington DC, United States, vol. 18, 2003.

[6] N. H. Kim and R. L. Webb, "Air-side heat transfer and friction correlations for plain fin-and-tube heat exchangers with staggered tube arrangements," *Journal of Heat Transfer*, vol. 121, pp. 662–667, 1999.

[7] M. Tutar and A. Akkoca, "Numerical analysis of fluid flow and heat transfer characteristics in three-dimensional plate fin-and-tube heat exchangers," *Numerical Heat Transfer, Part A: Applications*, vol. 46, no. 3, pp. 301–321, 2004.

[8] K. Park, D. H. Choi, and K. S. Lee, "Optimum design of plate heat exchanger with staggered pin arrays," *Numerical Heat Transfer, Part A: Applications*, vol. 45, no. 4, pp. 347–361, 2004.

[9] K. Torikoshi and G. Xi, "A numerical study of flow and thermal fields in finned tube heat exchangers (effect of the tube diameter)," in *Proceedings of the ASME Heat Transfer Division*, San Francisco, CA, USA, 1995, vol. 317-1, pp. 453–457.

[10] S. Tang and K.-T. Yang, "Thermal performance of a single-row fin-and-tube heat exchanger," *Journal of Thermal Science*, vol. 14, no. 2, pp. 172–180, 2005.

[11] E. Gianolio and F. Cuti, "Heat transfer coefficients and pressure drops for air coolers with different numbers of rows under induced and forced draft," *Heat Transfer Engineering*, vol. 3, no. 1, pp. 38–48, 1981.

[12] Watel B, Harmand S, and Desmet B, "Influence of flow velocity and fin spacing on forced convective heat transfer from an annular finned tube," *JSME International Journal Series B Fluids and Thermal Engineering*, vol. 42, no. 1, pp. 56–63, 1999.

[13] M. S. Mon and U. Gross, "Numerical study of fin-spacing effects in annular-finned tube heat exchangers," *International Journal of Heat and Mass Transfer*, vol. 47, no. 8–9, pp. 1953–1964, 2004.

[14] T. W. H. Sheui, S. F. Tsai, and T. P. Chiang, "Numerical study of heat transfer in two-row heat exchangers having extended fin surfaces," *Numerical Heat Transfer, Part A: Applications*, vol. 35, no. 7, pp. 797–814, 1999.

[15] H. Bilirgen, S. Dunbar, and E. K. Levy, "Numerical modeling of finned heat exchangers," *Applied Thermal Engineering*, vol. 61, no. 2, pp. 278–288, 2013.

[16] Taler D, "Experimental and numerical predictions of the heat transfer correlations in the cross-flow plate fin and tube heat exchangers," *Archives of Thermodynamics*, vol. 28, no. 1, pp. 3–18, 2007.

[17] H. T. Chen, J. C. Chou, and H. C. Wang, "Estimation of heat transfer coefficient on the vertical plate fin of finned-tube heat exchangers for various air speeds and fin spacings," *International Journal of Heat and Mass Transfer*, vol. 50, no. 1–2, pp. 45–57, 2007.

[18] G. Schüz and V. Kottke, "Visualization of flow, heat and mass transfer on finned tubes in cross flow," in *Flow Visualization IV*: *Proceedings of the Fourth International Symposium*, Paris, France, pp. 637–642, 1986.

[19] B. Kundu and P. K. Das, "Performance analysis and optimization of eccentric annular disk fins," *Journal of Heat Transfer*, vol. 121, no. 1, pp. 128–135, Feb. 1999.

[20] B. Kundu and P. K. Das, "Performance analysis and optimization of elliptic fins circumscribing a circular tube," *International Journal of Heat and Mass Transfer*, vol. 50, no. 1–2, pp. 173–180, 2007.

[21] A. H. Benmachiche, F. Tahrour, F. Aissaoui, M. Aksas and C. Bougriou, "Comparison of thermal and hydraulic performances of eccentric and concentric annular-fins of heat exchanger tubes," *Heat and Mass Transfer*, vol. 53, no. 8, pp. 2461–2471, 2001.

[22] A. H. Benmachiche, C. Bougriou, F. Tahrour, and M. Aksas, "3-D numerical study and comparison of eccentric and concentric annular-finned tube heat exchangers Numerical simulation of forced convection heat transfer for annular finned tube heat exchangers.," *Journal of Engineering Science and Technology*, vol. 10, no. 11, pp. 1508–1524, 2015.

[23] M. Shah and R. Shah, "Numerical investigation to analyse the effect of fin shape on performance of finned tube heat exchanger," *Journal of Mechanical Engineering and Sciences*, vol. 16, no. 3, pp. 9014–9024, 2022.

[24] H. Nemati, A. R. Rahimzadeh, and C. chuan Wang, "Heat transfer simulation of annular elliptical fin-and-tube heat exchanger by transition SST model," *Journal of Central South University*, vol. 27, no. 8, pp. 2324–2337, 2020.

[25] R. K. Banerjee, M. Karve, J. H. Ha, D. H. Lee, and Y. I. Cho, "Evaluation of enhanced heat transfer within a four row finned tube array of an air cooled steam condenser," *Numerical Heat Transfer, Part A: Applications*, vol. 61, no. 10, pp. 735–753, 2012.

[26] D. H. Lee, J. M. Jung, J. H. Ha, and Y. I. Cho, "Improvement of heat transfer with perforated circular holes in finned tubes of air-cooled heat exchanger," *International Communications in Heat and Mass Transfer*, vol. 39, no. 2, pp. 161–166, 2012.

[27] Y.A. Cengel, *Heat and Mass Transfer-A Practical Approach*, 3rd ed., McGraw-Hill, 2007.